Nat. Hazards Earth Syst. Sci. Discuss., 1, C2992–C3008, 2014
www.nat-hazards-earth-syst-sci-discuss.net/1/C2992/2014/

Natural Hazards and Earth System Sciences
Discussions

Interactive comment on "Source model of 18 September 2004 Huntoon Valley earthquake estimated from InSAR" *by* W. J. Lee et al.

W. J. Lee et al.

lu@usgs.gov

Received and published: 10 April 2014

We thank reviewer E. Trasatti for the very useful and constructive comments which have improved the quality of the manuscript.

-Major Point-

Q1. Two earthquakes? Bell et al. (2008) documented a M 5.4 (18 Sept. 2004), M5.6 (18 Sept. 2004) and a M 5.0 (20 Sept. 2004) earthquakes at Adobe Hills (Fig 3 of the technical report). I checked in the global-CMT and Neic-USGS catalogues, finding in both catalogues two earthquakes of the same magnitude in 18 Sept 2004, 5.4 at 23:02 GMT and 5.4 at 23:43 GMT, therefore at a very close distance. Even if we neglect the M 5.0 indicated by Bell et al. (2008), why authors avoid to clarify this

important point? They indicate the 23:02 earthquake only. It is obvious that InSAR cannot discern between the coseismic deformation due to the first or second earthquake since they happened in the same day with a time lapse of 40 minutes. The manuscript should be re-organized to take into account this important feature, since the deformation observed is cumulative, and the subsequent fault inversion will be related to both earthquakes.

A1. From the NCAeeDD catalog, there were three earthquakes with Mw > 5.0 on 18 Sept, 2004. However, the amount of ground surface deformation produced by an earthquake is highly controlled by its magnitude and depth (Okada, 1985). So we focused our research on the MW 5.6 event. Accordingly, we added the following sentences in the revised version: "NCAeeDD catalog reported three earthquakes: Mw 5.6 (3.26 km depth), MW 5.2 (7.15 km depth), and MW 5.4 (8.76 km depth). Generally, ground surface deformation produced by an earthquake is highly controlled by its magnitude and depth (Okada, 1985). Moreover, based on the simulation study of Dawson et al. (2007), InSAR is generally insensitive to the deformation of an earthquake with magnitude less than 5.5 and depth larger than 6 km. The surface deformation from the Mw5.6 earthquake is much larger than the combined deformation from the other two events. So, the observed deformation is mainly due to the Mw 5.6 event. Therefore, in this study, we focused on the Mw 5.6 earthquake which occurred at 23:02:17 (UTC) and compared the InSAR-derived source model parameters with those from the Mw 5.6 event."

Q2. InSAR data. The temporal baselines, especially for the ascending component, are very large. Authors don't show single interferograms, and don't discuss many aspects of the interferometric results. What about the coherence of interferograms with 1000 days of Btemp? Is the deformation distributed in the same way in all the interferograms? And there is a conceptual problem: how can be averaged different images. They contain post-seismic deformation also.Furthermore, as indicated in Section 3.3, during 2004-2006 there was a seismic rate increment. My suggestion is to show the In-

SAR images (not only the average), discuss coherence/results, clarifying which images are averaged.

A2. The study area maintains InSAR coherence higher than 0.3 even when the perpendicular baseline or the temporal baseline is large. Based on the reviewer's comment, we added coherence/interferogram figures (Fig 3 and Fig 4) and the following sentences in the revised manuscript: "The coherence of a repeat-pass interferogram highly depends on its perpendicular and temporal baselines. Fortunately, the study area maintains interferometric coherence value greater than 0.3 in spite of large perpendicular baseline and/or temporal baseline (Tables 2 and 3). This is because that Huntoon Valley is located in an arid semi-desert region with little vegetation. Fig. 3 shows coherence images which were calculated from original (not filtered) interferograms. Clearly, Fig. 3(b) and Fig. 3(d) have higher coherence because of short perpendicular or temporal baselines (Table 2). Other interferogram pairs used in this study have coherence value greater than 0.3 (Fig 3). The higher coherence of interferograms in this study allowed us to interpret the deformation results reliably."

"Then, we analyzed the interferograms (Figure 4) to ensure the observed signal is real deformation other than atmospheric artefacts. Indeed, most of the descending interferograms are noisy, including some atmospheric influences. However, the signals with lobe patterns persist in all the interferograms were unlikely due to atmospheric artifacts, because some interferograms were produced from independent SAR images acquired on different dates (e.g. Fig. 4a, 4c, 4g, 4i). Considering some of the interferograms were contaminated by atmospheric artifacts, we then carried out stacking method (Biggs et al., 2007) to obtain the co-seismic deformation by reducing atmospheric noise. Stacking is a technique that can extract subtle deformation signals out of multiple interferograms. By averaging many interferograms over the same area, random noise such as atmospheric signals can be subdued (Biggs et al., 2007). For earthquakes of this size, it should be noted that the postseimic deformation is negligible compared to the co-seismic part (Segall, 2010). Thus, in this study, the stacked

interferogram is dominated by the co-seismic deformation."

"Deformation time series that include the pre-, co-, post-seismic deformation results are shown in Fig. 8. We plotted the time-series displacements over two points (P1, P2) which have the maximum deformation from the ascending and descending tracks, respectively. In lieu of typical SBAS accuracy of 5.6 mm (Casu et al., 2006), the pre- and post-seismic deformation can't be distinguished outside the coseismic part due to the poor temporal-resolution of SAR datasets as well as the relatively small size of the earthquake (Fig. 8). So, the postseismic deformation, if any, should be included in the coseismic interferograms."

Q3. InSAR data for modeling. The images used in the modeling are downsampled? What is the associated error?

A3. Usually, deformation interferograms are downsampled to reduce the number of independent pixels to facilitate deformation modeling, particularly for large-area coseismic deformation field (e.g., Jonsson, 2002). In our case, we didn't downsample the InSAR data during the modeling. The earthquake is a moderate-size event, generating a maximum displacement of 2$\sim$3 cm only over an area of about 10 km by 10km. Therefore, it is not necessary to downsample the interferograms.

Q4. Conclusions. I believe the discussion about the importance of InSAR for determining source parameters are beyond the scope of the manuscript since this cannot be demonstrated by a basic finite fault with uniform slip inversion. In addition to the fact that the InSAR is pertinent to (at least) two earthquakes of comparable magnitude, while the seismic catalogues distinguish between them. I suggest the main scope of the manuscript should be the study the Huntoon valley earthquake giving new insights from InSAR and fault modeling.

A4. We made changes to reflect the reviewer's concerns (see the sections on '3.2 Comparison of source parameters from InSAR and seismology' and '4 Conclusions'). Indeed, due to the low temporal resolution of SAR data, it is impossible to detect post-

seismic deformation from InSAR datasets used in this study. Also, we used SBAS InSAR algorithm to increase the temporal sampling of the deformation time series, and added a new subsection 3.1 'Time-series deformation'.

Q5. Model information missing. The fault should be reported in one of the figures. Data error is missing. Goodness of fit not discussed quantitatively (RMS or % of residuals within errors).

A5. We added the following sentences: "RMS misfits are 6 mm and 4 mm for the descending-track and ascending-track interferograms, respectively.

Q6. P 4292 line 23. Better say "Agree within errors". Parameters uncertainty should be reported (InSAR and from seismic catalogues, usually available).

A6. For this earthquake, uncertainties for the earthquake catalogs are not available. We added the uncertainties for the modeled parameters in Table 4.

Q7. Section 3.3. There is no "suspect" (line 18) but certainty that InSAR images contain cumulative cosesimic deformations of the three (or two) earthquakes of similar magnitude. See arguments of points 1 and 2. This section should be re-organized accordingly.

A7. Please refer to responses to Q 1 and Q 4.

-Minor Point-

Q1. P 4288. both "SAR" may be removed at line 3.

A1. Removed.

Q2. 4288 line 6. "obvious" to be removed.

A2. Removed.

Q3. 4288 lines 11-12. "images: : :tracks" may be removed.

A3. Removed.

Q4. – P 4288 lines 17-19 last phrase is unsupported by rigorous analysis, should be removed. Geodetic inversions by single fault with uniform slip is very basic and the estimated depth is often shallower than from seismic inversions since the deformation data is relative to the free surface. Before going to this conclusion, a quantitative analysis of fault parameters estimation from geodetic and/or seismic analysis should be performed, and this is beyond the purpose of the present manuscript, I guess. Accordingly, also the discussion/conclusions should be modified.

A4. Because these are a sequence of small earthquakes and a single fault model can fit the InSAR data very well, it is not necessary to use a complex model. To address the reviewer's concerns, we made changes in this section.

Q5. P 4289 lines 5-6. "and: : :strong" to be removed.

A5. Removed.

Q6.P 4289 line 17. InSAR acronym defined few lines above.

A6. Removed.

Q7. P 4289 line 26. "without further modeling" what does it mean?

A7. Removed.

Q8. P 4291 line 5. "u" is a vector or a matrix? Because u_asc and u_dsc seem to be two vectors. What is "r"?

A8. u is the unit LOS deformation vector. To clarify r and u vectors, we added the following sentences: "u is a matrix containing unit LOS vectors (u_asc, u_dsc) which can be calculated based on the corresponding θ and φ from the ascending and descending tracks, respectively. r is a vector representing the LOS deformation measurements (observations) from interferograms of both ascending and descending tracks"

Q9. P 4292 line 7. "reasonably well" is unsupported by quantitative data, e.g. RMS or percentual of residuals between data error.

A9. We replaced the sentence with the following: “RMS misfits are 4 mm and 6 mm for the ascending and descending interferograms, respectively. The descending interferogram has a slightly larger RMS misfit than the ascending one due to relatively stronger atmospheric artifacts in the descending interferograms.”

Q10. P 4292 from line 19. Institute acronyms should be defined in the text before first citation of Table 1 or in the table caption.

A10. Institute acronyms were moved to introduction

Q11. P 4293 lines 9-10. Conclusion should be reviewed taking into account the uncertainties of the retrieved source parameters.

A11. We added uncertainties for the model parameters in Table 4.

Q12. P4295 line 19. “Last access” necessary?

A12. Removed.

Q13. P4296 Table 1. Please use same number of significant digit. Refer to text for acronyms definition, or insert acronyms here. All the longitudes must have same sign (negative).

A13. Fixed

Q14. P4299 Table 4. Negative longitude. Errors missing!

A14. Fixed

Q15. P4300 Fig 1. Mw + 5.5 may become Mw 5.5.

A15. Fixed.

Q16. P4301 Fig 2. Mm instead of rad should be better.

A16. Fixed.

Please also note the supplement to this comment:
http://www.nat-hazards-earth-syst-sci-discuss.net/1/C2992/2014/nhessd-1-C2992-2014-supplement.pdf

---

Interactive comment on Nat. Hazards Earth Syst. Sci. Discuss., 1, 4287, 2013.

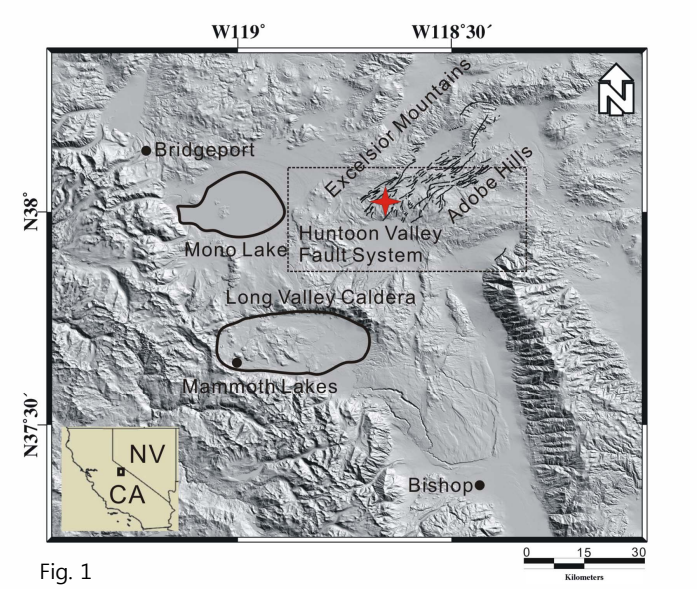

Fig. 1. Shaded relief map of Huntoon Valley and surroundings.

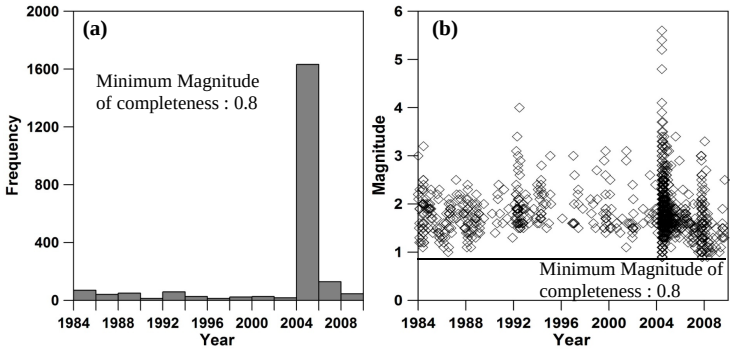

Fig. 2. Distribution of (a) frequency and (b) magnitude of earthquakes occurred near the Huntoon Valley area from NCAeqDD catalog

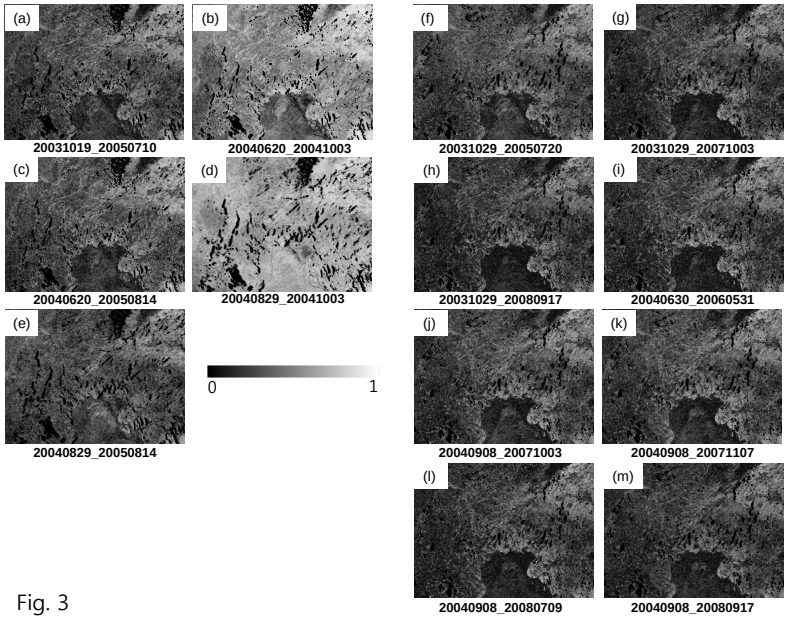

Fig. 3

Fig. 3. Coherence maps

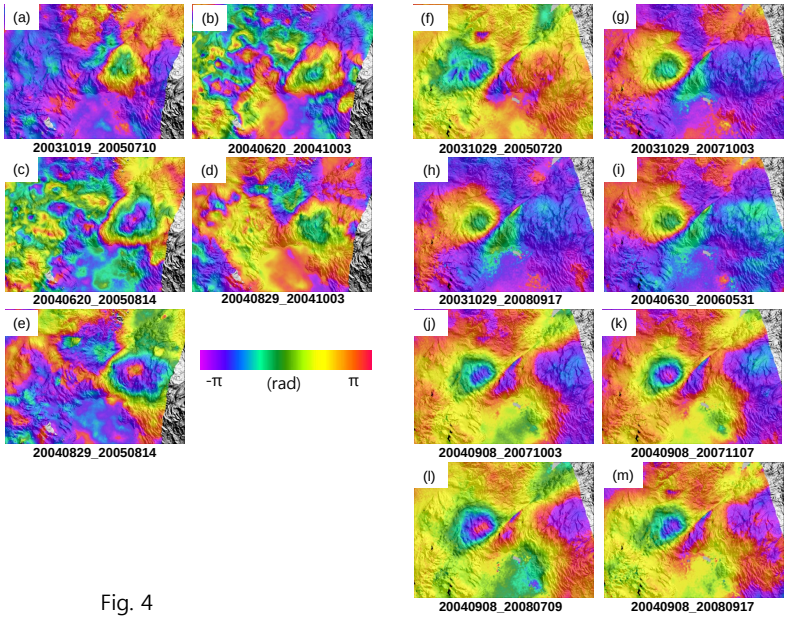

Fig. 4

Fig. 4. Wrapped Interferogram

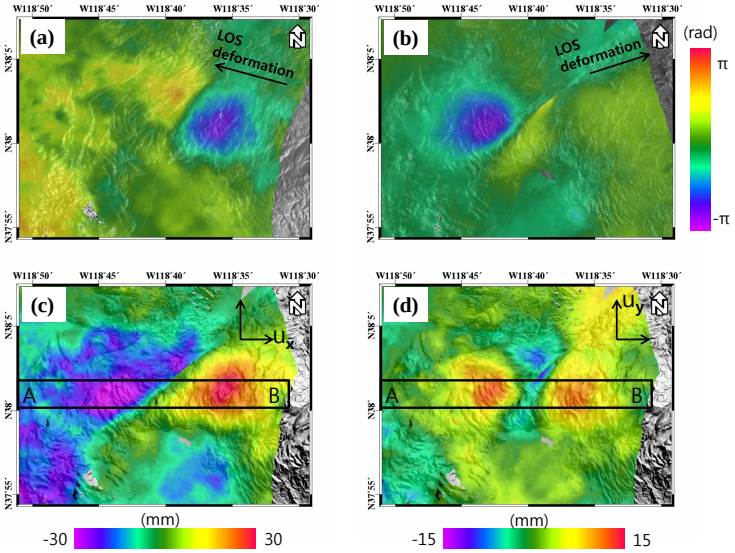

Fig. 5

Fig. 5. deformation images

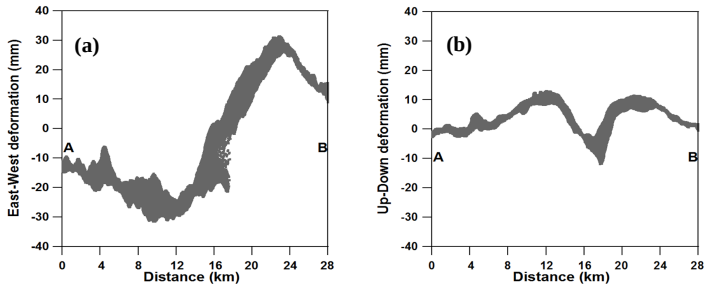

Fig. 6

Fig. 6. East-west (a) and vertical (b) components of the deformation

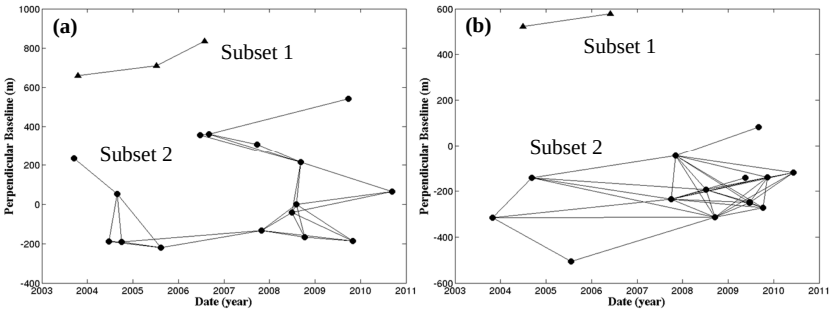

Fig. 7

Fig. 7. Perpendicular baselines used for SBAS InSAR processing

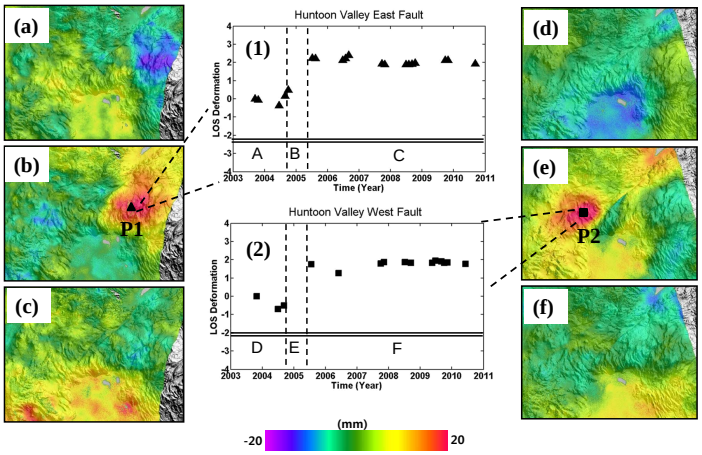

Fig. 8

Fig. 8. Time-series surface deformation

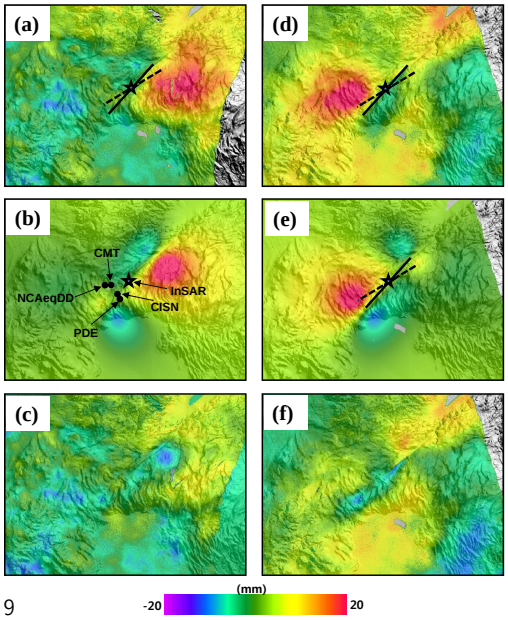

Fig. 9

Fig. 9. Observed & modelled deformation images